

Quantitative evaluation of local pulmonary distribution of TiO₂ in rats following single or multiple intratracheal administrations of TiO₂ nanoparticles using X-ray fluorescence microscopy

Guihua Zhang^a, Naohide Shinohara^{a*}, Hirokazu Kano^b, Hideki Senoh^b, Masaaki Suzuki^b, Takeshi Sasaki^c, Shoji Fukushima^b and Masashi Gamo^a

ABSTRACT: Uneven pulmonary nanoparticle (NP) distribution has been described when using single-dose intratracheal administration tests. Multiple-dose intratracheal administrations with small quantities of NPs are expected to improve the unevenness of each dose. The differences in local pulmonary NP distribution (called microdistribution) between single- and multiple-dose administrations may cause differential pulmonary responses; however, this has not been evaluated. Here, we quantitatively evaluated the pulmonary microdistribution (per mesh: 100 $\mu\text{m} \times 100 \mu\text{m}$) of TiO₂ in lung sections from rats following one, two, three, or four doses of TiO₂ NPs at a same total dosage of 10 mg kg⁻¹ using X-ray fluorescence microscopy. The results indicate that: (i) multiple-dose administrations show lower variations in TiO₂ content (ng mesh⁻¹) for sections of each lobe; (ii) TiO₂ appears to be deposited more in the right caudal and accessory lobes located downstream of the administration direction of NP suspensions, and less so in the right middle lobes, irrespective of the number of doses; (iii) there are not prominent differences in the pattern of pulmonary TiO₂ microdistribution between rats following single and multiple doses of TiO₂ NPs. Additionally, the estimation of pulmonary TiO₂ deposition for multiple-dose administrations imply that every dose of TiO₂ would be randomly deposited only in part of the fixed 30–50% of lung areas. The evidence suggests that multiple-dose administrations do not offer remarkable advantages over single-dose administration on the pulmonary NP microdistribution, although multiple-dose administrations may reduce variations in the TiO₂ content for each lung lobe. Copyright © 2016 John Wiley & Sons, Ltd.

Additional supporting information may be found in the online version of this article at the publisher's web-site.

Keywords: intratracheal administration; multiple doses; local pulmonary NP deposition; TiO₂; XRF

Introduction

With increased application of nanoparticles (NPs) in diverse fields, there have been growing concerns about the safety of these nanomaterials. Intratracheal administration tests have been conducted for toxicological assessment of inhaled NPs (Jacobsen *et al.*, 2009; Sun *et al.*, 2012), and there are some advantages to this method: (i) the actual dose delivered to experimental animals is reproducible; (ii) the protocol is easier to perform and at far lower cost compared with the inhalation exposure protocol, which requires aerosol generation of large amounts of NPs and inhalation chamber construction; and (iii) it permits the introduction of large and effective doses of nanomaterials in a short time.

Although single-dose administration is often performed (He *et al.*, 2010; Shinohara *et al.*, 2014), some studies have described the uneven distribution of NPs in the lung when using single-dose intratracheal administration tests (Brain *et al.*, 1976; Leong *et al.*, 1998; Zhang *et al.*, 2015). It is expected that multiple doses of small quantities of the NPs would improve the unevenness of each dose and result in a more even distribution in the lung, which would be more similar to the condition in the inhalation exposure study. Brain *et al.* (1976) reported that

multiple-dose administrations reduced the unevenness of pulmonary particle distribution compared with single-dose administration. In the study, they administered ^{99m}Tc-S-colloid particles to hamsters, divided the lung lobes of each hamster into 54 pieces and measured the deposition of ^{99m}Tc particles in each lung piece. Then, they observed that numbers of the lung pieces, which have an extremely high deposition of ^{99m}Tc particles, were decreased and the interlobar deposition differences were reduced.

In terms of toxicological evaluation of the NPs, the microscopic histopathological examinations were often performed in local pulmonary areas using thin lung sections (Sun *et al.*, 2012; Yoshiura

*Correspondence to: Naohide Shinohara, National Institute of Advanced Industrial Science and Technology (AIST), Tsukuba, Ibaraki 305-8569, Japan.
E-mail: n-shinohara@aist.go.jp

^aNational Institute of Advanced Industrial Science and Technology (AIST), Tsukuba, Ibaraki 305-8569, Japan

^bJapan Bioassay Research Center, Hadano, Kanagawa 257-0015, Japan

^cNational Institute of Advanced Industrial Science and Technology (AIST), Tsukuba, Ibaraki 305-8565, Japan

et al., 2015). Thus, it is anticipated that differences in the local pulmonary NP distribution in a microscopic scale, which is termed microdistribution hereafter, between single- and multiple-dose administrations, if any, may cause differential pulmonary responses to the administered NPs; this, however, has not yet been evaluated.

Microbeam X-ray fluorescence (XRF) analysis is an elemental analysis technique that allows for the examination of quite a small area of the sample, and it has been applied for the evaluation of the microdistribution of NP in biological samples (Wang *et al.*, 2007, 2008). However, few studies have quantitatively evaluated the microdistribution of NPs due to there being no suitable reference samples. For this reason, we have successfully developed a new set of Ti reference samples and applied these to evaluate quantitatively the pulmonary microdistribution (per mesh: 100 $\mu\text{m} \times 100 \mu\text{m}$) of TiO_2 in rats administered intratracheally with a single dose of TiO_2 NPs (Zhang *et al.*, 2015).

The present study is aimed to investigate differences in the pattern of pulmonary microdistribution of TiO_2 between single- and multiple-dose administrations. To this end, we quantitatively evaluated the pulmonary microdistribution of TiO_2 in the sections of lungs from rats administered intratracheally with one, two, three, or four doses of TiO_2 NPs at a total dosage of 10 mg kg^{-1} body weight, using microbeam XRF microscopy. We used TiO_2 NPs because it is one of the most popular nanomaterials applied in biomedicine (Yin *et al.*, 2013), cosmetics (Su *et al.*, 2014) and environmental engineering (Khodadoust *et al.*, 2012).

Materials and methods

Preparation of TiO_2 suspension

In the current study, AEROSIL® P25 (Nippon Aerosil Co., Ltd, Tokyo, Japan) was used to prepare the suspension of TiO_2 NPs. AEROSIL® P25 has a spherical primary particle size of 21 nm, with a mixture of anatase and rutile phases in a 80 : 20 ratio. The actual value of primary particle size of P25 was 24 ± 7.9 (mean \pm SD) using transmission electron microscopy (JEM-2010; Japan Electro Optical Laboratory Ltd., Tokyo, Japan), and the specific surface of P25 was $59 \text{ m}^2 \text{ g}^{-1}$. The details for preparation of P25 stock suspension were described in our previous study (Zhang *et al.*, 2015). A part of this stock suspension was diluted two-, three- and four-fold with disodium phosphate solution (2 mg ml^{-1}). The concentrations of P25 stock and diluted suspensions were measured to be 10.3, 5.26, 3.58 and 2.73 mg ml^{-1} , respectively, using a weight scale after drying the suspension in a thermostatic chamber (ON-300S; AS ONE Co., Japan). The average particle sizes of P25 suspensions were determined to be 72 nm (for 10.3 mg ml^{-1}), 90 nm (for 5.26 mg ml^{-1}), 79 nm (for 3.58 mg ml^{-1}) and 82 nm (for 2.73 mg ml^{-1}), using DLS (Zetasizer nano-ZS; Malvern Instruments Ltd., UK). These data indicated no significant agglomeration with the changing concentrations of P25 suspensions.

Animal husbandry

Male F344/DuCrIj rats (SPF) were obtained at the age of 11 weeks from Charles River Laboratories Japan, Inc. (Kanagawa, Japan). The animals were quarantined and acclimated for 8 days. All animals were housed individually in stainless-steel wire hanging cages (170 mm [W] \times 294 mm [D] \times 176 mm [H]) under controlled environmental conditions (temperature of $23 \pm 2 \text{ }^\circ\text{C}$ and relative humidity of $55\% \pm 15\%$ with 15–17 air changes h^{-1}) in

barrier-controlled animal rooms. Fluorescent lighting was controlled automatically to provide a 12 h light/dark cycle. All rats had free access to sterilized water and a γ -irradiation-sterilized commercial basal diet (CRF-1; Oriental Yeast Co., Ltd., Tokyo, Japan). The animals were cared for in accordance with the guidelines for the care and use of laboratory animals (NRC, 1996), and the experimental protocol was approved by the Institutional Animal Care and Use Committee at the Japan Bioassay Research Center.

Experimental design and intratracheal administration

The experimental design of this study is shown in Fig. 1. The total dosage of TiO_2 NPs was set relatively high (10 mg kg^{-1} body weight) for the purpose of Ti quantitative analysis in the present study. The rats were divided into four groups (five rats, each) for one (10 mg kg^{-1} body weight \times 1), two (5.0 mg kg^{-1} body weight \times 2), three (3.3 mg kg^{-1} body weight \times 3), and four doses (2.5 mg kg^{-1} body weight \times 4) of TiO_2 NPs at a total dosage of 10 mg kg^{-1} body weight. The rats were treated once every other day. The body weight was measured immediately before the first administration of the TiO_2 suspension and found to be $256 \pm 9 \text{ g}$ (mean \pm SD). After inhalational anesthesia with 2.5% isoflurane gas (Forane; Abbott Japan Co., Ltd., Tokyo, Japan), the rats were administered intratracheally the suspensions of TiO_2 NPs (1 ml kg^{-1} body weight) using a MicroSprayer Aerosolizer (Model IA-1B; Penn-Century, Inc., Wyndmoor, PA, USA). The MicroSprayer was inserted 25 mm from the larynx (near the tracheal bifurcation) of the rat. In addition, in a preliminary test, we indicated that the recovery rate of TiO_2 was $86\% \pm 17\%$ (mean \pm SD) in the lung lobes of rats, administered intratracheally with the same dose of TiO_2 NPs using the MicroSprayer the day after the NP administration. It suggested that most administered TiO_2 NPs could reach the pulmonary region, and a token portion of TiO_2 NPs may have been cleared by the ciliary motility in airways 1 day after the administration.

The rats were euthanized by exsanguination from the abdominal aorta when under intraperitoneal pentobarbital anesthesia, the day after the last NP administration for each group, and the left and right cranial, middle, caudal, and accessory lobes were separately removed. Next, 3 μm thick sections were prepared from the paraffin-embedded lung lobes, and the sections were mounted onto glass slides without glass coverslips (due to a considerably high detection of Ti [about five-fold of maximal Ti

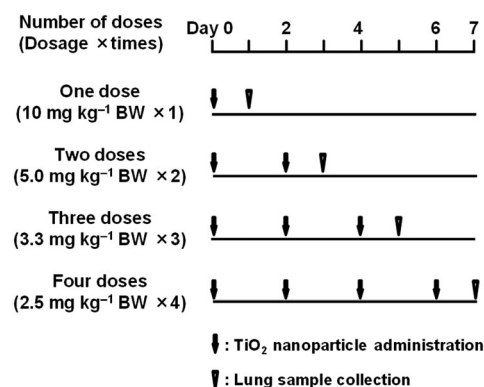


Figure 1. Experimental design of single (one dose) and multiple (two, three, and four doses) intratracheal administrations of AEROSIL® P25 TiO_2 nanoparticle at a total dosage of 10 mg kg^{-1} BW in male F344 rats aged 12 weeks ($n = 5$ for each dose test). The administration was performed every other day, and the rats were dissected on the following day after the last administration of TiO_2 nanoparticle. BW, body weight.

content in the lung sections of rats administered with TiO₂ NPs] in glass coverslips) and stained with hematoxylin and eosin. Untreated rats (control) were also euthanized, and lung sections of the left and right lobes were prepared under the same conditions as described above. The details of intratracheal administration and lung section preparation were as described in our previous study (Zhang *et al.*, 2015).

Quantification of pulmonary TiO₂ microdistribution using X-ray fluorescence microscopy

The spectral intensities of Ti in the samples were measured with a high-performance energy-dispersive XRF microscopy with a rhodium target X-ray tube (XGT-7200; Horiba Int., Kyoto, Japan). The spectral intensity of the Ti-K α line (4.511 keV) was acquired for the quantification of Ti in selected rectangular areas of the samples. The analytical conditions of Ti were set as follows: beam size (spatial resolution), 100 μm ; step size, 200 μm for lung sections from the control and TiO₂-treated rats; acquisition time, 60 s point⁻¹; excited voltage, 50 kV; excited current, 1 mA; full vacuum mode. The spectral intensity of Ti in a mesh (100 μm \times 100 μm) was measured for each analytical point.

Our previous study (Zhang *et al.*, 2015) have described the preparation and analysis of Ti reference samples (step size: 100 μm) for the Ti calibration curve. In addition, we indicated the accuracy and validity for the quantification of pulmonary TiO₂ deposition using the developed quantitative method, which has the main features of (i) excellent linearity between the intensity of Ti and the content of Ti ($R^2 = 0.999$), and (ii) ensured high data reproducibility by correction of a calibration curve using a Ti reference sample at least once every 2 months and the recalibration of the calibration curve after replacement of the X-ray tube.

The net spectral intensity of each analysis point in the sections of each lung lobe from rats administered with one, two, three, or four doses of TiO₂ NPs was calculated using the following equation:

$$I_{\text{net of each analytical point (cps)}} = I_n - I_{\text{bg}} \quad (1)$$

where $I_{\text{net of each analytical point}}$ is the Ti net spectral intensity of each analytical point; I_n is the Ti measured spectral intensity of each analytical point; and I_{bg} is the average Ti spectral intensity of the background. Because similar Ti spectral intensities were observed in the lung sections from untreated rats and the glass slides, the area of the glass slide that was adjacent to the lung section was used instead of the lung sections of untreated rat as the background. The content of TiO₂ in the mesh (100 μm \times 100 μm) was quantified based on the Ti calibration curve obtained from the Ti reference samples.

Derivation of the detection limit of TiO₂

The content of TiO₂ NPs for each lung section from untreated rats (control, $n = 3$) was calculated from the spectral intensities of Ti measured with XRF microscopy in the lung section. Based on the maximum value of the SD (SD_{max}) of the data obtained in lung sections, the detection limit of TiO₂ was defined as three-fold SD_{max} .

Statistical analysis

All statistical analyses were performed using SPSS software (IBM SPSS Statistics version 20; IBM Corp., Armonk, NY, USA). A one-way analysis of variance with Tukey's HSD test was used to

compare: (i) the content and detection rates of TiO₂ in the sections of each lung lobe or the entire lung lobe among the rats after one, two, three, and four doses; (ii) the content and detection rates of TiO₂ among the sections of five lung lobes in rats administered with the same dose of TiO₂ NPs; and (iii) the frequencies of TiO₂ detection at each of six content ranges of TiO₂ for the sections of each lobe among the rats receiving one, two, three, and four doses of TiO₂ NPs. $P < 0.05$ was used as the criterion for statistical significance.

Results

Detection limit of TiO₂

The SDs of the TiO₂ content in the mesh (100 μm \times 100 μm) were 0.019–0.021 ng mesh⁻¹ for the sections of right cranial, middle, caudal, accessory, and left lobes from the untreated rats (control, $n = 3$). Based on a three-fold SD_{max} value (i.e., 0.021 ng mesh⁻¹) obtained from lung sections of the untreated rats, the detection limit of TiO₂ was estimated to be 0.063 ng mesh⁻¹ (6.3 ng mm⁻²).

Quantitative evaluation of pulmonary microdistribution of TiO₂

The content and the detection rates of TiO₂ in sections of lung lobes from the untreated rats (control, $n = 3$) and rats administered with one, two, three, or four doses of TiO₂ NPs at a total dosage of 10 mg kg⁻¹ body weight ($n = 5$ for each dose), are presented in Table 1. The representative quantitative maps of the pulmonary TiO₂ microdistribution are shown in Fig. 2 (all maps in Supplementary information Figs S1–S4). The directions of lung sections shown in Fig. 2 represent the actual directions of lung lobes when the rats were administered intratracheally with suspensions of the TiO₂ NPs (the direction of arrows represented the lung hilum where the suspension of TiO₂ NPs entered the lung). TiO₂ was rarely detected in the sections of all lung lobes from the untreated rats (e.g., the detection rates of TiO₂ were $< 0.30\%$).

In terms of pulmonary TiO₂ microdistribution in the sections of each lung lobe between single- and multiple-dose administrations, there were no significant differences in the content (including the mean, 95th percentile and maximum content) or the detection rates of TiO₂ for the sections of almost each lung lobe among the rats receiving one, two, three, and four doses of TiO₂ NPs (Table 1). Although there were significant differences in the maximum content of TiO₂ for the sections of right cranial (1.5 ng mesh⁻¹ for one dose vs 0.85 ng mesh⁻¹ for two doses) or entire lung lobes (1.5 ng mesh⁻¹ for one dose vs 0.92–1.1 ng mesh⁻¹ for multiple doses) between the rats administered with single and multiple doses of TiO₂ NPs ($P < 0.05$), these differences were less than two-fold.

Concerning the pulmonary TiO₂ microdistribution among sections of lung lobes for each dose, there were higher levels in the mean content, 95th percentile content and detection rates of TiO₂ for the right caudal, right accessory and left lobes, and higher values in the maximum content of TiO₂ for the right caudal and accessory lobes compared with the right middle lobes, irrespective of number of doses, although statistically different from the right middle lobes, were not always observed. It should be noted that only one rat (Rat No.5) administered with a single dose of TiO₂ NPs showed an opposite trend of TiO₂ deposition where there was a higher mean content of TiO₂ in the right cranial and middle

Table 1. Data relating to the pulmonary quantitative microdistribution (per 100 $\mu\text{m} \times 100 \mu\text{m}$ mesh, step size: 200 μm) of TiO_2 in sections of right and left lung lobes from the untreated rats (control, $n = 3$), and the rats administered intratracheally with one, two, three or four doses of AEROSIL® P25 TiO_2 nanoparticles at a total dosage of 10 mg kg^{-1} body weight ($n = 5$ for each dose)

| Lung section | Parameter | Control | One dose | Two doses | Three doses | Four doses |
|--------------|--|---|--|--|--|---|
| Right | Cranial | | | | | |
| | Content of TiO_2 (ng mesh ⁻¹) | Mean \pm SD 95th percentile Maximum | 0.000 ND 0.085 \pm 0.031 0.10 \pm 0.032 | 0.073 \pm 0.039 0.47 \pm 0.24 1.5 \pm 0.42 22 \pm 5.2 | 0.047 \pm 0.016 ^{ab} 0.29 \pm 0.070 ^{ab} 0.85 \pm 0.14 ^{ab,*} 21 \pm 6.6 ^{ab} | 0.043 \pm 0.0099 ^b 0.29 \pm 0.072 ^b 1.1 \pm 0.24 19 \pm 2.5 ^a |
| Middle | Detection rate of TiO_2 (%) | Mean \pm SD | 0.000 | 0.045 \pm 0.049 | 0.015 \pm 0.013 ^a | 0.024 \pm 0.013 ^a |
| | Content of TiO_2 (ng mesh ⁻¹) | 95th percentile Maximum | ND 0.076 \pm 0.0064 0.14 \pm 0.028 | 0.34 \pm 0.37 1.2 \pm 0.82 13 \pm 5.2 | 0.10 \pm 0.099 ^a 0.46 \pm 0.25 ^a 9.0 \pm 6.5 ^a | 0.21 \pm 0.043 ^b 1.0 \pm 0.24 15 \pm 4.3 ^a |
| Caudal | Detection rate of TiO_2 (%) | Mean \pm SD | 0.000 | 0.10 \pm 0.051 | 0.077 \pm 0.014 ^{ab} | 0.061 \pm 0.017 ^{ab} |
| | Content of TiO_2 (ng mesh ⁻¹) | 95th percentile Maximum | ND 0.11 \pm 0.020 0.17 \pm 0.088 | 0.55 \pm 0.23 2.0 \pm 0.99 29 \pm 9.4 | 0.40 \pm 0.10 ^{ab} 1.0 \pm 0.29 ^{ab} 32 \pm 4.6 ^b | 0.32 \pm 0.065 ^b 1.3 \pm 0.62 29 \pm 6.6 ^b |
| Accessory | Detection rate of TiO_2 (%) | Mean \pm SD | 0.000 | 0.086 \pm 0.075 | 0.087 \pm 0.084 ^{ab} | 0.088 \pm 0.024 ^b |
| | Content of TiO_2 (ng mesh ⁻¹) | 95th percentile Maximum | ND 0.074 \pm 0.0055 0.20 \pm 0.098 | 0.45 \pm 0.36 1.6 \pm 0.75 24 \pm 15 | 0.36 \pm 0.28 ^{ab} 0.97 \pm 0.46 ^{ab} 31 \pm 22 ^b | 0.48 \pm 0.13 ^a 1.4 \pm 0.35 38 \pm 4.9 ^b |
| Left | Detection rate of TiO_2 (%) | Mean \pm SD | 0.000 | 0.065 \pm 0.066 | 0.11 \pm 0.041 ^b | 0.086 \pm 0.031 ^b |
| | Content of TiO_2 (ng mesh ⁻¹) | 95th percentile Maximum | ND 0.077 \pm 0.0064 0.22 \pm 0.040 | 0.38 \pm 0.33 1.1 \pm 0.57 22 \pm 9.0 | 0.49 \pm 0.19 ^b 1.3 \pm 0.50 ^b 40 \pm 4.7 ^{b,*} | 0.32 \pm 0.070 ^b 0.96 \pm 0.32 30 \pm 6.0 ^b |
| Entire lung | Detection rate of TiO_2 (%) | Mean \pm SD | 0.000 | 0.075 \pm 0.021 | 0.071 \pm 0.013 | 0.060 \pm 0.0075 |
| | Content of TiO_2 (ng mesh ⁻¹) | 95th percentile Maximum | ND 0.084 \pm 0.0024 0.17 \pm 0.036 | 0.44 \pm 0.13 1.5 \pm 0.25 22 \pm 1.9 | 0.33 \pm 0.052 0.92 \pm 0.037 [*] 26 \pm 7.5 | 0.33 \pm 0.042 1.1 \pm 0.22 [*] 26 \pm 0.89 |

^aND, not detectable.

^bData indicated as ND are calculated as 0 ng mesh⁻¹. The detection limit of TiO_2 is 0.063 ng mesh⁻¹ (per 100 $\mu\text{m} \times 100 \mu\text{m}$ mesh). The detection rate of TiO_2 is the percentage of the detected analytical points to all analytical points of Ti in each lung section.

^cSignificant differences ($P < 0.05$) on the content and detection rates of TiO_2 among the sections of five lung lobes for each dose are shown by completely different letters that are not sharing a letter (e.g. a and b or c).

* Significantly different from one dose ($P < 0.05$).

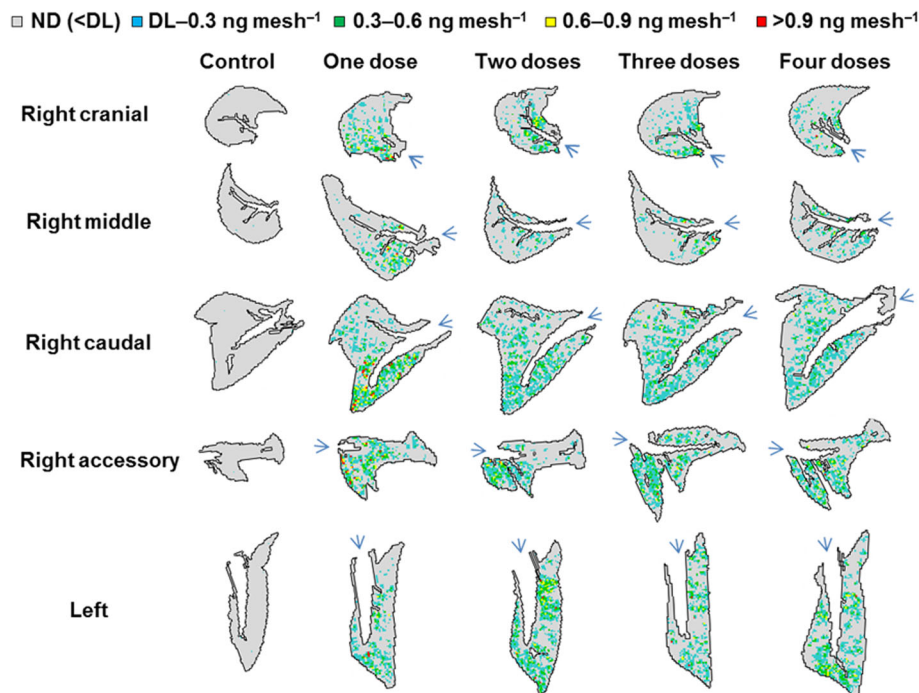


Figure 2. Representative quantitative maps of the pulmonary microdistribution of TiO₂ in sections of right and left lung lobes from the untreated rats ($n = 3$), and the rats administered intratracheally with one, two, three and four doses of AEROSIL® P25 TiO₂ NPs at a total dosage of 10 mg kg⁻¹ body weight ($n = 5$ for each dose test), using X-ray fluorescence microscopy (XGT-7200). The DL of TiO₂ was 0.063 ng mesh⁻¹. The suspension of TiO₂ NPs entered the lung through the lung hilum (the direction of arrows). The direction of lung sections represents the actual direction of lung lobes when the rats were administered with the suspension of TiO₂ NPs. ND, not detectable; DL, detection limit; NPs, nanoparticles.

lobes than in the right caudal and accessory lobes (Supplementary information Fig. S1).

The frequencies of TiO₂ detection at each of the six content ranges (including detection limit (DL)–0.2, 0.2–0.4, 0.4–0.6, 0.6–0.8, 0.8–1.0, and > 1.0 ng mesh⁻¹) of TiO₂ for the sections of lung lobes

from the rats administered intratracheally with one, two, three, or four doses of TiO₂ NPs are plotted in Fig. 3. The sections of each lobe or entire lung lobes showed similar frequencies of TiO₂ detection at almost each content range among the rats following one, two, three, and four doses of TiO₂ NPs. Although single-dose

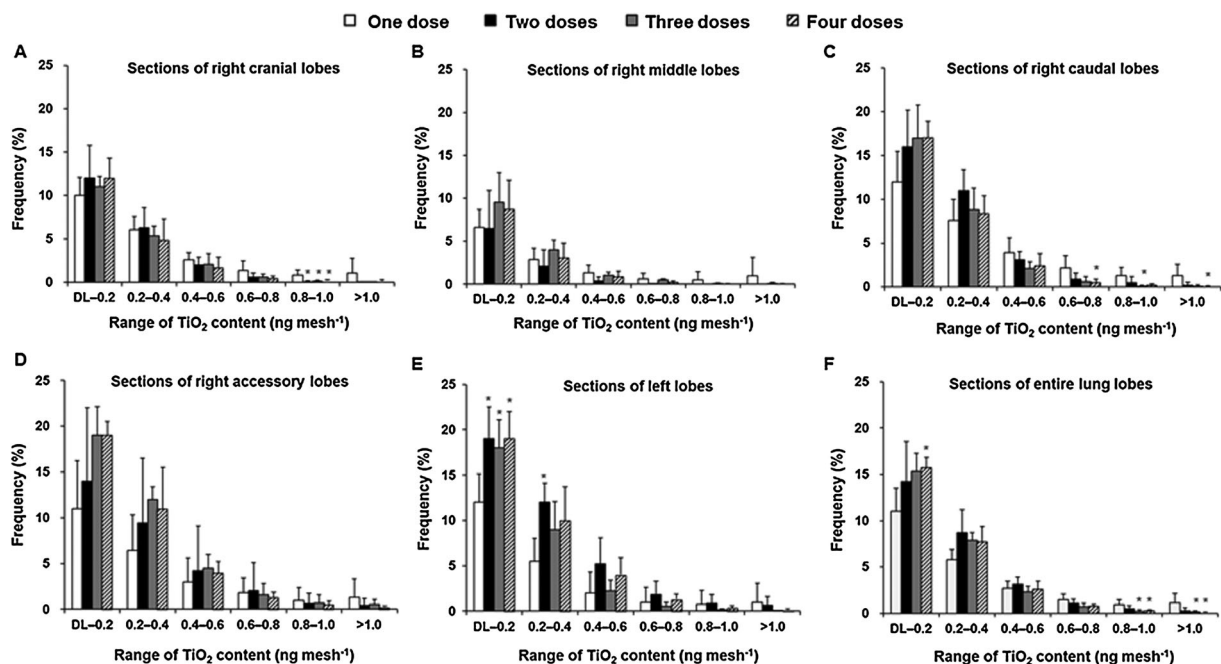


Figure 3. The frequencies of TiO₂ detection at each of the six content ranges of TiO₂ for the sections of each lung lobe (A: right cranial lobes; B: right middle lobes; C: right caudal lobes; D: right accessory lobes; E: left lobes; F: entire lung lobes) from the rats following one, two, three and four doses of AEROSIL® P25 TiO₂ nanoparticles at a total dosage of 10 mg kg⁻¹ body weight ($n = 5$ for each dose test). * $P < 0.05$ compared to one dose. DL, detection limit.

administration showed significantly higher frequencies of TiO₂ detection at relatively higher content ranges in the right cranial (Fig. 3A), right caudal (Fig. 3C) or entire lung lobes (Fig. 3F) than multiple-dose administrations ($P < 0.05$), the values regarding the frequencies of TiO₂ detection were quite low at each of those higher content ranges (e.g., right cranial lobe: 0.84% for one vs 0.094–0.19% for two, three or four doses at the content range of 0.8–1.0 ng mesh⁻¹; right caudal lobe: 1.3–2.2% for one vs 0.060–0.52% for three or four doses at each of the content ranges above 0.6 ng mesh⁻¹; entire lung lobe: 0.90–1.1% for one dose vs 0.10–0.25% for three or four doses at each of the content ranges above 0.8 ng mesh⁻¹). There were significantly lower frequencies of TiO₂ detection at the lower content ranges of TiO₂ in the sections of left lobes (Fig. 3E) and entire lung lobes (Fig. 3F) in rats following a single dose compared with those receiving multiple doses of TiO₂ NPs.

Furthermore, the coefficients of variation in the mean content of TiO₂ in a mesh for sections of the right cranial, middle, caudal, accessory or left lung lobes from rats administered with the same dose of TiO₂ NPs ($n = 5$) were, respectively, 54.2%, 107%, 50.4%, 87.3%, and 102% for one dose; 35.2%, 83.4%, 18.2%, 97.0%, and 37.1% for two doses; 23.0%, 27.5%, 26.2%, 30.1%, and 30.2% for three doses; and 47.0%, 53.6%, 27.2%, 27.1%, and 36.7% for four doses. These data indicate large variations in the sections of each lung lobe among rats treated with the same dose. However, the variations appear to decrease when correlated with an increasing number of doses.

Discussion

In the present study, we quantitatively evaluated the pulmonary TiO₂ microdistribution in rats administered intratracheally with one, two, three, or four doses of TiO₂ NPs at the same total dosage of 10 mg kg⁻¹ body weight using XRF microscopy to investigate differences in the pattern of the local pulmonary NP distribution between single- and multiple-dose administrations.

In the present study, Ti was rarely detected in sections of all the lung lobes from the untreated rats (control), demonstrating the existence of low Ti in the lungs of untreated rats. The detected Ti can represent the administered TiO₂ because TiO₂ NPs are insoluble particles, and the Ti background was very small.

The data on the pulmonary microdistribution of TiO₂ (Table 1) suggest that similar content (ng mesh⁻¹) and frequencies of TiO₂ were deposited in each lung lobe among the rats following single, two, three, and four doses of TiO₂ NPs. For a detailed pulmonary microdistribution of TiO₂ (Fig. 3), the frequencies of TiO₂ detection were also similar at almost each of the content ranges for each lung lobe among the rats administered with one, two, three, and four doses of TiO₂ NPs. Higher frequencies of TiO₂ detection were observed at relatively higher content ranges (> 0.6 ng mesh⁻¹) for the sections of each lung lobe in rats following one dose than those receiving multiple doses of TiO₂ NPs. This result appears in accordance with the observation of Brain *et al.* (1976) that multiple-dose administrations decreased the frequencies of an extremely high deposition of ^{99m}Tc particles in the lungs. However, these differences are not considered to affect significantly the pulmonary microdistribution of TiO₂ due to quite low values at these content ranges (e.g., > 0.6 ng mesh⁻¹ for the entire lung; 3.5% for one dose; and 1.1–1.8% for multiple doses). Moreover, we did not observe remarkable differences in the 95th percentile and maximum content of TiO₂ for the sections of almost each lung lobe between the rats following single and multiple doses of TiO₂ NPs. The

results regarding the pulmonary microdistribution of TiO₂ NPs indicate that a large single dose did not result in prominent regions of a high concentration of TiO₂ deposition in the lung compared with multiple smaller doses of TiO₂ NPs at the same total dosage, suggesting that improvement in the unevenness of the pulmonary distribution of TiO₂ NPs with multiple-dose administrations is limited. In addition, the pulmonary deposition of TiO₂ for multiple-dose administrations of TiO₂ NPs was estimated using the pulmonary TiO₂ deposition data of single-dose administration measured in the present study, under four assumptions: (i) every dose of TiO₂ NPs would be randomly deposited in the entire lung area (Fig. 4A); (ii) 50% of lung (Fig. 4B); (iii) 30% of lung (Fig. 4C); or (iv) deposited only in the same meshes with a different content of TiO₂ (Fig. 4D). The estimated results of pulmonary TiO₂ deposition suggest that every dose of TiO₂ would be randomly deposited only in part of the fixed 30–50% of lung areas even if TiO₂ NPs were administered with multiple doses for the intratracheal administration tests.

Reasor and Antonini (2001) reported that only minor differences in the pulmonary responses were observed between the rats receiving a single large and multiple smaller intratracheal administrations of crystalline silica. In the current study, the prominent differences in the pattern of pulmonary TiO₂ microdistribution are not observed in rats following single and multiple doses of TiO₂ NPs (P25), which are the same insoluble particles as silica. Considering the pulmonary responses to the administered particles may be related to the pattern of pulmonary microdistribution of TiO₂, these observations are consistent. Although significantly lower frequencies of TiO₂ detection were observed at certain lower content ranges of TiO₂ in the left lobes or entire lung lobes from the rats following a single dose compared with those receiving multiple doses of TiO₂ NPs, this difference might not significantly affect pulmonary responses owing to the relatively lower content values of TiO₂ at these ranges.

Our results suggest that TiO₂ appears to be deposited more in the right caudal and accessory lobes, which were located downstream of the direction of administration of the NP suspensions in rats following a single dose of TiO₂ NPs. It is consistent with the results of Brain *et al.* (1976) and Leong *et al.* (1998) in which similar deposition trends of the particles (^{99m}Tc or dye) were seen among the lung lobes in rats receiving a single-dose administration of the particles. We indicate that multiple-dose administrations do not change the interlobar deposition trend of TiO₂ compared with the single-dose administration at the same total dosage of TiO₂ NPs. Brain *et al.* (1976) also reported a similar deposition trend among the lung lobes of hamsters administered intratracheally with multiple doses of ^{99m}Tc-S-colloid particles, despite multiple-dose administrations appeared to improve partially the unevenness of the interlobar particle distribution. Moreover, more TiO₂ appears to be distributed in the lower portion of each lung lobe (Fig. 2) in rats receiving single or multiple doses of TiO₂ NPs. This is supported by a study by Brain *et al.* (1976) in which single or multiple doses of labeled particles (^{99m}Tc) resulted in less deposition in the apical areas and greater amounts in basal regions of each lung lobe.

Furthermore, variations in the mean content of TiO₂ for the sections of each lung lobe among the rats treated with the same dose appear to decrease, which is inversely correlated with the increase in the number of doses (coefficients of variation ($n = 5$): 54.2–107% for single dose vs 27.1–53.6% for four doses). This is also agreed with the observation of Brain *et al.* (1976) in which multiple-dose administrations of ^{99m}Tc-S-colloid particles decreased the variation in the particle deposition among the samples of each lung lobe in

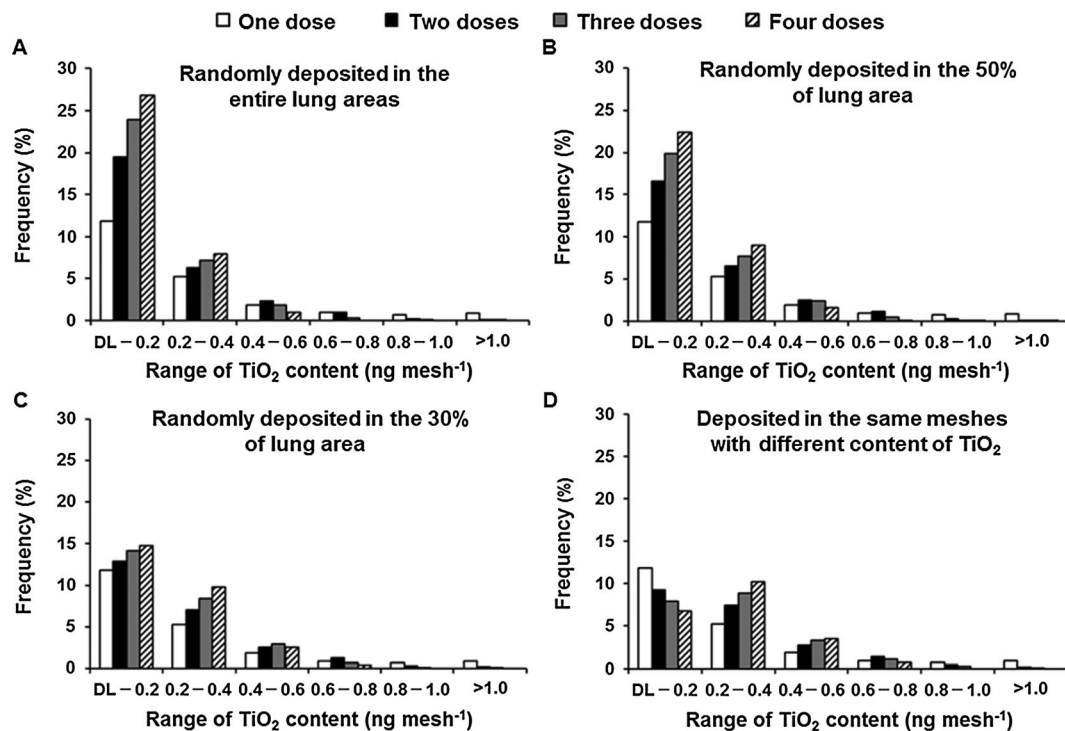


Figure 4. The estimation of pulmonary TiO₂ deposition for multiple-dose administrations of AEROSIL® P25 TiO₂ nanoparticles using the pulmonary TiO₂ deposition data of single-dose administration measured in the present study, under four assumptions: (i) every dose of TiO₂ nanoparticles would be randomly deposited in the entire lung area (A); (ii) 50% of lung areas (B); (iii) 30% of lung areas (C); or (iv) deposited only in the same meshes with different content of TiO₂ (D). DL, detection limit.

hamsters (coefficients of variation: 45.7–85.2% for single vs 23.8–43.8% for multiple). These observations suggest that multiple-dose administrations decrease variation in the content of TiO₂ for each lung lobe among rats with the same dose compared with single-dose administration.

In conclusion, we quantitatively evaluated the pulmonary microdistribution of TiO₂ in rats administered intratracheally with one, two, three, or four doses of TiO₂ NPs at a total dosage of 10 mg kg⁻¹ body weight. Our results indicate that improvement in the unevenness of the pulmonary distribution of NPs with multiple-dose administrations is limited, and there are no prominent differences in the pattern of the pulmonary microdistribution of TiO₂ between the rats following single and multiple doses of TiO₂ NPs. Moreover, the estimation of pulmonary TiO₂ deposition implied that every dose of TiO₂ would be randomly deposited only in part of the fixed 30–50% of lung areas even if multiple-dose administrations were conducted for the intratracheal administration tests. The evidence suggests that multiple-dose administrations do not offer remarkable advantages over single-dose administration with respect to the local pulmonary distribution of TiO₂.

Acknowledgments

We wish to thank Ms. Tomoko Yanagibashi for preparing the pulmonary microdistribution maps of TiO₂. This work is part of the research program entitled “Development of innovative methodology for safety assessment of industrial nanomaterials,” supported by the Ministry of Economy, trade and Industry (METI) of Japan.

Conflict of interest

The authors did not report any conflict of interest.

References

- Brain JD, Knudson DE, Sorokin SP, Davis MA. 1976. Pulmonary distribution of particles given by intratracheal instillation or by aerosol inhalation. *Environ. Res.* **11**: 13–33.
- He X, Zhang H, Ma Y, Bai W, Zhang Z, Lu K, Zhao Y, Chai Z. 2010. Lung deposition and extrapulmonary translocation of nano-ceria after intratracheal instillation. *Nanotechnology* **21**: 285103.
- Jacobsen NR, Moller P, Jensen KA, Vogel U, Ladefoged O, Loft S, Wallin H. 2009. Lung inflammation and genotoxicity following pulmonary exposure to nanoparticles in ApoE(-/-) mice. *Part. Fibre Toxicol.* **6**: 2.
- Khodadoust S, Sheini A, Armand N. 2012. Photocatalytic degradation of monoethanolamine in waste water using nanosized TiO₂ loaded on clinoptilolite. *Spectrochim. Acta A* **92**: 91–95.
- Leong BKJ, Coombs JK, Sabaitis CP, Rop DA, Aaron CS. 1998. Quantitative morphometric analysis of pulmonary deposition of aerosol particles inhaled via intratracheal nebulization, intratracheal instillation or nose-only inhalation in rats. *J. Appl. Toxicol.* **18**: 149–160.
- NRC. 1996. *Guide for the Care and Use of Laboratory Animals*. National Research Council, National Academy Press: Washington, DC.
- Reasor MJ, Antonini JM. 2001. Pulmonary responses to single versus multiple intratracheal instillation of silica in rats. *J. Toxicol. Environ. Health A* **12**(62): 9–21.
- Shinohara N, Oshima Y, Kobayashi T, Imatanaka N, Nakai N, Ichinose T, Sasaki T, Zhang G, Fukui H, Gamo M. 2014. Dose-dependent clearance kinetics of intratracheally administered titanium dioxide nanoparticles in rat lung. *Toxicology* **325**: 1–11.
- Su CY, Tang HZ, Zhu GD, Li CC, Lin CK. 2014. The optical properties and sun-screen application of spherical h-BN-TiO₂/mica composite powder. *Ceram. Int.* **40**: 4691–4696.
- Sun QQ, Tan DN, Ze YG, Sang XZ, Liu XR, Gui SX, Cheng Z, Cheng J, Hu R, Gao G, Liu G, Zhu M, Zhao X, Sheng L, Wang L, Tang M, Hong F. 2012. Pulmotoxicological effects caused by long-term titanium dioxide nanoparticles exposure in mice. *J. Hazard. Mater.* **235–236**: 47–53.
- Wang JX, Chen CY, Yu HW, Sun J, Li B, Li YF, Gao YX, He W, Huang YY, Chai ZF, Zhao YL, Deng XY, Sun HF. 2007. Distribution of TiO₂ particles in the olfactory bulb of mice after nasal inhalation using microbeam SRXRF mapping techniques. *J. Radioanal. Nucl. Chem.* **272**: 527–531.

Wang JX, Chen CY, Liu Y, Jiao F, Li W, Lao F, Li YF, Li B, Ge C, Zhou G, Gao Y, Zhao Y, Chai Z. 2008. Potential neurological lesion after nasal instillation of TiO₂ Nanoparticles in the anatase and rutile crystal phases. *Toxicol. Lett.* **183**: 72–80.

Yin ZF, Wu L, Yang HG, Su YH. 2013. Recent progress in biomedical applications of titanium dioxide. *Phys. Chem. Chem. Phys.* **15**: 4844–4858.

Yoshiura Y, Izumi H, Oyabu T, Hashiba M, Kambara T, Mizuguchi Y, Lee BW, Okada T, Tomonaga T, Myojo T, Yamamoto K, Kitajima S, Horie M, Kuroda E, Morimoto Y. 2015. Pulmonary toxicity of well-dispersed titanium dioxide nanoparticles following intratracheal instillation. *J. Nanopart. Res.* **17**: 241.

Zhang G, Shinohara N, Kano H, Senoh H, Suzuki M, Sasaki T, Fukushima S, Gamo M. 2015. Quantitative evaluation of the pulmonary microdistribution of TiO₂ nanoparticles using XRF microscopy after intratracheal administration with a microsyringe in rats. *J. Appl. Toxicol.* **35**: 623–630.

Supporting information

Additional supporting information may be found in the online version of this article at the publisher's web-site.